**Atmospheric
Chemistry
and Physics**

Validation of ACE-FTS v2.2 methane profiles from the upper troposphere to the lower mesosphere

M. De Mazière[1], **C. Vigouroux**[1], **P. F. Bernath**[2,14], **P. Baron**[3], **T. Blumenstock**[4], **C. Boone**[2], **C. Brogniez**[5], **V. Catoire**[6], **M. Coffey**[7], **P. Duchatelet**[8], **D. Griffith**[9], **J. Hannigan**[7], **Y. Kasai**[3], **I. Kramer**[4], **N. Jones**[9], **E. Mahieu**[8], **G. L. Manney**[10,15], **C. Piccolo**[11], **C. Randall**[16], **C. Robert**[6], **C. Senten**[1], **K. Strong**[12], **J. Taylor**[12], **C. Tétard**[5], **K. A. Walker**[2,12], **and S. Wood**[13]

[1]Belgian Institute for Space Aeronomy (BIRA-IASB), Brussels, Belgium
[2]Department of Chemistry, University of Waterloo, Waterloo, Ontario, Canada
[3]National Institute of Information and Communications Technology (NICT), Tokyo, Japan
[4]IMK-ASF, Forschungszentrum Karlsruhe and University Karlsruhe, Karlsruhe, Germany
[5]Laboratoire d'Optique Atmosphérique, Université des sciences et technologies de Lille, Lille, France
[6]Laboratoire de Physique et Chimie de l'Environnement, CNRS – Université d'Orléans, Orléans, France
[7]National Center for Atmospheric Research (NCAR), Boulder, CO, USA
[8]Institut d'Astrophysique et de Géophysique, Université de Liège, Liège, Belgium
[9]School of Chemistry, University of Wollongong, Wollongong, Australia
[10]Jet Propulsion Laboratory, California Institute of Technology, Pasadena, CA, USA
[11]Atmospheric, Oceanic and Planetary Physics, University of Oxford, Oxford, UK
[12]Department of Physics, University of Toronto, Toronto, Ontario, Canada
[13]National Institute of Water and Atmospheric Research (NIWA), Lauder, New-Zealand
[14]Department of Chemistry, University of York, Heslington, York, UK
[15]New Mexico Institute of Mining and Technology, Socorro, NM, USA
[16]Laboratory for Atmospheric and Space Physics and Department of Atmospheric and Oceanic Sciences, University of Colorado, Boulder, CO, USA

Abstract. The ACE-FTS (Atmospheric Chemistry Experiment – Fourier Transform Spectrometer) solar occultation instrument that was launched onboard the Canadian SCISAT-1 satellite in August 2003 is measuring vertical profiles from the upper troposphere to the lower mesosphere for a large number of atmospheric constituents. Methane is one of the key species. The version v2.2 data of the ACE-FTS CH_4 data have been compared to correlative satellite, balloon-borne and ground-based Fourier transform infrared remote sensing data to assess their quality. The comparison results indicate that the accuracy of the data is within 10% in the upper troposphere – lower stratosphere, and within 25% in the middle and higher stratosphere up to the lower mesosphere (<60 km). The observed differences are generally consistent with reported systematic uncertainties. ACE-FTS is also shown to reproduce the variability of methane in the stratosphere and lower mesosphere.

1 Introduction

Methane (CH_4) is the most abundant organic trace gas in the atmosphere. It is the only atmospheric organic compound that has a sufficiently long lifetime (of the order of 8 to 10 years) to be transported from the troposphere to the stratosphere. A discussion of the global cycle of methane can be found, e.g., in Wahlen (1993) and Brasseur et al. (1999). In the troposphere, the volume mixing ratio (VMR) of methane is quite uniform. Yet there is a clear interhemispheric gradient, with present-day VMR values of about 1.7 ppmv in the Southern Hemisphere (SH) and about 1.85 ppmv in the Northern Hemisphere (NH) (GLOBALVIEW-CH4, 2005). This gradient reflects the larger sources of methane in the NH. Thus air entering the stratosphere contains approximately these amounts of methane. The methane abundance also shows a distinct seasonal variation: the net effect of larger sources and stronger chemical losses (see further below) in warmer months gives rise to the largest concentrations in local winter and the lowest concentrations in local summer. The amplitude of the seasonal cycle is largest in the

northern high latitudes (30–40 ppb) and diminishes towards the equator. It is smaller in the SH (10–20 ppb) where it is quite constant with latitude (Wahlen, 1993).

A common destruction mechanism for methane in the stratosphere and the troposphere is reaction with OH, forming the methyl radical CH_3 and water vapour (H_2O). Additional sinks in the stratosphere are the reactions with $O(^1D)$ or Cl atoms, forming CH_3 and OH or HCl, respectively. Methane is therefore a sink for chlorine atoms in the stratosphere, hence its importance in stratospheric ozone chemistry, and a source of stratospheric water vapour. Chemical destruction of methane in the lower stratosphere is quite slow, because of the low abundances of $O(^1D)$ and Cl atoms, and because of the strong temperature dependence of the reaction with OH. Therefore in the low stratosphere, the CH_4 VMR can be used as a tracer of dynamical processes.

In the troposphere, methane is of great importance in tropospheric chemistry, as it usually is the most abundant and certainly the most ubiquitous hydrocarbon. Its oxidation scheme, starting with the reaction with OH, ultimately produces CO_2. A major intermediate in the degradation of CH_4 is formaldehyde (H_2CO). Other oxidation products are carbon monoxide (CO), and, in the presence of elevated NO_x concentrations, ozone.

Sources of methane are oxygen-deficient wetland habitats such as swamps, lakes, tundra, and boreal marshes. Methane is also produced in soils and oceans, as an end product of the decomposition of organic material. The rate of methane production is highest in tropical wetlands. Methane is also released by anaerobic microbial activity in the stomachs of cattle, termites, and perhaps other insects. Important anthropogenic sources are coal mining, biomass burning, natural gas losses and solid waste burning, as well as cultivation of rice paddies.

Among the most important reasons to measure the concentration of methane is the fact that it is the third most important greenhouse gas in the atmosphere (after water vapour and CO_2) and that its concentration has almost doubled since preindustrial times, from 0.975 ppmv to 1.85 ppmv (Northern Hemisphere).

On a per molecule basis, methane has a much greater climate warming potential than CO_2.

Methane is one of the key target species for the Atmospheric Chemistry Experiment-Fourier Transform Spectrometer (ACE-FTS) instrument that was launched in August 2003. CH_4 vertical profiles covering the upper troposphere to mesosphere have been retrieved from the ACE-FTS measurements and need to be validated using independent correlative data, which is the subject of the present paper. More information about the ACE mission and the CH_4 retrievals is given in Sect. 2. What we call validation of the ACE-FTS measurements is their comparison with independent data sets that have been characterised earlier and that can therefore be considered reference data sets. The result of such a validation is a characterisation of this new data set relative to known

data sets. Similarly, when we use the word bias in the paper, we are talking about a systematic deviation of the ACE-FTS data set relative to the known reference data set.

Available observations of CH_4 include the in situ surface networks, in particular, the NOAA/ESRL Global Monitoring Network (http://www.esrl.noaa.gov/gmd/), and the ground-based infrared remote sensing instruments, e.g., in the framework of the Network for Detection of Atmospheric Composition Change (NDACC, http://www.ndacc.org; formerly called NDSC, for Network for the Detection of Stratospheric Change), that have provided long-term systematic high-quality measurements since the early eighties. The former ones provide only local surface data. The latter provide low-resolution vertical profile information and are therefore useful for comparison to the ACE-FTS data, as will be further discussed in Sect. 3.

High vertical resolution profile measurements in the stratosphere and mesosphere, sometimes down to the upper troposphere, have been obtained using satellite-borne limb sounding infrared spectral instruments. Among such earlier satellite experiments is the Atmospheric Trace Molecule Spectroscopy experiment (ATMOS). It is a Fourier-transform solar occultation infrared spectrometer (http://remus.jpl.nasa.gov/atmos) that was deployed four times on the Space Shuttle (April, 1985, March, 1992, April, 1993 and November, 1994), and that can be considered a predecessor of the ACE-FTS instrument (Gunson et al., 1990 and 1996; Abrams et al., 1996). Following ATMOS, observations of CH_4 vertical profiles in the stratosphere and upper troposphere have been carried out by the ISAMS (Improved Stratospheric and Mesospheric Sounder) (Remedios et al., 1996), CLAES (Cryogenic Limb Array Etalon Spectrometer) (Roche et al., 1996) and HALOE (Halogen Occultation Experiment) (Russell et al., 1993; Park et al., 1996) instruments onboard UARS, the Upper Atmosphere Research Satellite (http://uars.gsfc.nasa.gov/www_root/homepage/uars-science.html; Reber et al., 1993), that operated between mid-September 1991 and mid-December 2005. ISAMS and CLAES stopped observations in July 1992, and May 1993, respectively. HALOE (http://haloedata.larc.nasa.gov) provides the longest data set, covering the period 11 October 1991 to 21 November 2005, including a significant period of overlap with the ACE mission. HALOE measurements of CH_4 have been validated by Park et al. (1996). More information about the quality of the HALOE CH_4 data and the comparisons with the ACE-FTS data are given in Sect. 6.

More recently, other interesting global data sets for CH_4 are being provided by the SCIAMACHY (SCanning Imaging Absorption spectroMeter for Atmospheric CHartographY) and MIPAS (Michelson Interferometer for Passive Atmospheric Sounding) instruments onboard Envisat (Environmental Satellite) launched on 1 March 2002 (e.g., Frankenberg et al., 2005, and Raspollini, et al., 2006, respectively). However, the actual SCIAMACHY data sets for CH_4 provide

only total column information and therefore this data set is not useful for validation of the ACE-FTS vertical profile measurements. The MIPAS data set and its comparison with ACE-FTS are discussed in Sect. 5.

Presently, observations of tropospheric CH_4 are also carried out by AIRS (Atmospheric Infrared Sounder; http://www-airs.jpl.nasa.gov/; Barnet et al., 2003) onboard Aqua, launched on 4 May 2002, and by TES (Tropospheric Emission Spectrometer; http://tes.jpl.nasa.gov) onboard the AURA satellite, launched on 15 July 2004. At present, TES provides nadir data for CH_4 that are not validated yet for geophysical use. The AIRS nadir data for CH_4 provide essentially tropospheric column data (up to about 100 hPa) and therefore are not really suitable for comparison with the ACE-FTS vertical profile data. They provide however a very interesting complementary data set.

Measurements by balloon- and aircraft-borne remote- or in situ-sensing instruments provide information complementary to the satellite and ground-based instruments: in Sect. 4 of the present paper, we show data from the SPIRALE instrument and discuss their agreement with coincident ACE-FTS profiles.

A summary of the above mentioned individual validation efforts is discussed in Sect. 7, in which we also draw clear conclusions regarding the quality of the ACE-FTS CH_4 profile data. Once validated, the ACE-FTS CH_4 data set will constitute a very valuable extension of the time series made up of the ATMOS, HALOE and MIPAS data, starting in 1985, now covering more than 20 years of high vertical resolution methane distributions from the upper troposphere to the mesosphere on a global scale.

2 ACE-FTS measurements of CH_4

The ACE-FTS instrument was launched onboard the SCISAT-1 satellite of the Canadian Space Agency, on 13 August 2003. The satellite is in a high-inclination (74°) circular low-earth orbit (650 km from the surface). The ACE-FTS operates in solar occultation mode; the orbit provides a latitudinal coverage from 85° S to 85° N for these measurements. The instrument operates at a high spectral resolution of $0.02\,cm^{-1}$ in the range of 2.2 to 13.3 μm (750–4400 cm^{-1}). It provides measurements from the upper troposphere to about 150 km altitude, of temperature and pressure, of the atmospheric extinction, and of the concentrations of a large number of atmospheric species, with a vertical resolution of the order of 4 km. A description of the ACE mission can be found in Bernath et al. (2005).

Methane (CH_4) is one of the routinely retrieved target species of ACE-FTS. The retrieval algorithm has been described by Boone et al. (2005). The retrieval process starts with the derivation of pressure and temperature profiles which are then used in the retrieval of the VMR profiles of the atmospheric constituents. The VMR profile above the

Table 1. Microwindows used for the retrieval of CH_4 from the ACE-FTS spectra, as a function of retrieval altitude.

Center Wavenumber (cm^{-1})	Microwindow Width (cm^{-1})	Lower Altitude (km)	Upper Altitude (km)
1245.14	0.30	39	50
1267.78	0.30	45	60
1270.73	0.30	40	60
1283.43	0.30	50	70
1287.80	0.30	55	70
1299.89	0.30	40	55
1302.07	0.30	45	70
1302.74	0.30	55	70
1303.63	0.35	45	70
1304.25	0.30	40	60
1311.50	0.30	50	60
1322.08	0.30	38	70
1327.23	0.60	35	70
1332.08	0.30	55	70
1332.48	0.30	40	70
1332.75	0.30	55	70
1337.55	0.30	40	60
1341.68	0.35	35	70
1342.65	0.30	55	70
1346.65	0.40	32	57
1348.00	0.35	32	57
1350.95	0.30	30	55
1351.74	0.30	35	55
1353.10	0.40	33	60
1356.00	0.35	35	55
1407.60	0.30	15	30
1427.60	0.35	9	20
1439.43	0.35	10	25
1463.00	0.35	12	25
2610.20	0.35	10	27
2613.98	0.35	20	30
2614.73	0.30	20	33
2618.27	0.35	25	37
2622.58	0.30	20	33
2636.30	0.30	5	20
2644.72	0.35	12	28
2650.70	0.35	5	20
2658.08	0.35	12	28
2658.60	0.35	5	25
2664.50	0.35	17	30
2667.19	0.30	20	30
2667.47	0.35	10	27
2667.85	0.40	5	25
2669.65	0.30	5	20
2671.30	0.30	15	30
2671.66	0.45	5	25
2674.15	0.35	20	32
2675.62	0.30	12	27
2691.25	0.30	25	35
2805.97	0.30	23	33
2809.02	0.30	27	37
2820.82	0.30	25	40
2822.68	0.30	28	43
2825.05	0.30	28	40
2828.17	0.40	30	45
2835.61	0.35	18	31
2839.48	0.50	8	22
2841.22	0.35	15	30
2847.72	0.35	27	43
2849.25	0.30	25	36
2857.50	0.35	10	25
2867.10	0.30	30	40
2869.53	0.30	5	20
2888.48	0.28	25	39

Table 2. Identification of contributing ground-based FTIR stations.

Site	Latitude North (°)	Longitude East (°)	Responsible Institution
Thule	77	−69	NCAR
Kiruna	68	20	IMK-Karlsruhe
Poker Flat	65	−147	NICT
Jungfraujoch	47	8	Univ. Liège
Toronto	44	−79	Univ. Toronto
Izaña	28	−16	IMK-Karlsruhe
St. Denis at Ile de La Réunion	−21	55	BIRA-IASB
Wollongong	−34	151	Univ. Wollongong
Lauder	−45	170	NIWA
Arrival Heights	−78	167	NIWA

highest analyzed measurement is taken as a constant times the first-guess profile. First-guess profiles for the VMR retrievals are taken from the results of the ATMOS missions (Gunson et al., 1996). It is important to note that ACE-FTS retrievals are not sensitive to a priori information except for the shape of the first-guess profile above the highest analyzed measurement. ACE-FTS forward model calculations employ the HITRAN 2004 line list and cross sections (Rothman et al., 2005). For the retrieval of methane, in the ACE-FTS v2.2 processing, different microwindows have been used, as a function of altitude. They are listed in Table 1. Between 10 and 20 microwindows are used simultaneously at each altitude. The lower altitude limit of a microwindow is chosen to avoid saturation and, in some cases, interferences from other molecules. The upper altitude limit is where the depths of the target absorptions approach the measurement noise. For a molecule like methane it is impossible to use a single set of microwindows over the whole altitude range. In the chosen set of microwindows, there are no strong interferences. Minor interferences from CH_4 and CO_2 isotopologues ($^{13}CH_4$, $^{13}CO_2$, $CO^{18}O$), and from HDO (for occultations where atmospheric water levels are high) are included in the spectral simulations, but they are so small that there is little benefit in fitting them.

The ACE-FTS retrieved methane VMR profiles extend from the upper troposphere to the lower mesosphere (67 to 70 km altitude); the reported inversion errors in this altitude range are of the order of a few percent (2 to 3%), except at the lowest and highest altitude limits of the retrieval where they may rise to more than 10%.

It is worth noticing that in the microwindows used at low altitude, the CH_4 lines are affected by line mixing effects and deviate from the Voigt line shape due to collisional effects (Mondelain et al., 2007). These effects are not included in the ACE-FTS forward spectral model, and therefore may contribute to the errors in the retrievals at these altitudes.

3 Comparisons of ACE-FTS data with FTIR ground-based measurements of CH$_4$

3.1 Characteristics of the ground-based FTIR data set

Ground-based (g-b) data for methane have been derived from regularly performed solar absorption observations by high-spectral-resolution Fourier transform infrared (FTIR) spectrometers, in the framework of NDACC. The names and coordinates of the g-b NDACC stations that have contributed data for the validation of the ACE-FTS methane profiles are listed in Table 2. Good latitudinal coverage is obtained, going from the high Arctic to the Antarctic, including the subtropics. The FTIR data products are profiles with a low vertical resolution, of the order of 10 km, from the surface to an altitude of about 30 km. They are obtained from a spectral fitting procedure using the Optimal Estimation method (Rodgers, 2000), which uses a statistical weighting between a priori information and measurements. More information about the retrieval algorithms can be found in Hase et al. (2004) and references therein. The spectral microwindows, the a priori information and additional retrieval parameters have been optimised at each site as a function of the local conditions (altitude and latitude of the site, spectral data quality, etc.). All microwindows used are situated in the range of 2610 to 2925 cm^{-1}, which coincides with the range in which the microwindows for the ACE-FTS upper troposphere to middle stratosphere (30 km) retrievals are located – see Table 1. Consistently at all sites, HITRAN2004 spectroscopic parameters and Voigt lineshape functions have been used in the forward line-by-line spectra calculations, as was done for ACE-FTS retrievals. It is important to note that the uncertainties on the spectroscopic parameters of CH_4 are rather large, namely of the order of 20%. These uncertainties are a dominant source of systematic uncertainties in the retrieved profiles.

3.2 Comparison methodology

For the comparisons, we have required a temporal coincidence within ±24 h, and a spatial coincidence within ±1000 km. These criteria are quite relaxed, but acceptable for a species like CH_4 that has a long lifetime and is rather well mixed in the atmosphere. At the polar sites however, the criteria have been more severe. At Arrival Heights, we have used the additional requirement that the difference in potential vorticity (PV) between the observed airmasses (defined at the location of the station and the 30 km tangent point of the satellite profile) are smaller than 15%. At Kiruna, Thule and Poker Flat, we have required a temporal coincidence within ±12 h, and a spatial coincidence within ±500 km (for Kiruna and Thule) and within ±600 km at Poker Flat (with the ±500 km criterion, we had only 2 coincidences left).

The altitude range in which both instruments have good sensitivity is limited at the lower boundary by the ACE-FTS

Table 3. Comparisons between ACE-FTS and g-b FTIR partial columns (PC) in the upper troposphere-middle stratosphere at all contributing sites. N is the number of coincidences (for description of criteria: see text). DOF is the number of Degrees of Freedom for Signal. M is the mean of the differences between the ACE-FTS and g-b FTIR partial columns, in percentage, relative to the mean of the FTIR partial columns; STD is the 1σ standard deviation associated with the ensemble of comparisons, and SEM is the associated standard error on the mean, as explained in Sect. 3.2. Err is the combined random error on the difference between the ACE-FTS and FTIR partial columns, in percentage, relative to the mean of the FTIR profiles.

Site	ACE-FTS lower altitude (km)	PC limits (km)	N	DOF for PC	M±SEM (%)	STD (%)	Err (%)
Thule	7.7±2.4	12–33	13	1.5±0.0	0.3±1.5	5.4	3.1
Kiruna	8.9±1.9	13–26	12	1.0±0.2	3.0±1.6	5.6	2.5
Poker Flat	7.0±1.4	11–25	4	1.4±0.2	9.8±3.5	7.0	2.2
Jungfraujoch	10.1±3.0	13–25	26	0.9±0.1	0.6±0.7	3.4	2.5
Toronto	8.2±2.1	12–32	8	1.9±0.1	−12.1±2.2	6.0	2.5
Izaña	12.1±4.1	15–28	5	1.1±0.1	−6.2±2.9	6.7	2.3
St-Denis	6.8±1.5	12–29	4	0.9±0.0	−6.1±1.6	3.3	2.6
Wollongong	6.8±1.0	12–32	6	1.6±0.1	−4.4±3.6	8.9	3.0
Lauder	8.1±2.1	12–30	21	1.4±0.1	−7.8±1.1	4.7	2.6
Arrival Heights	7.7±2.0	12–30	19	1.3±0.1	−4.6±1.1	4.9	2.5
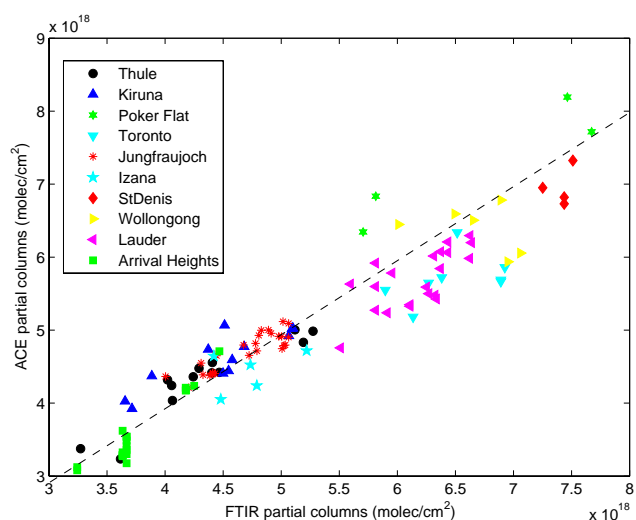
Fig. 1. Correlation plot of the ACE-FTS versus ground-based FTIR partial column amounts of methane considered in the comparisons summarized in Table 3, for all contributing stations. Different symbols refer to different stations, as indicated in the legend.

data and at the upper boundary by the g-b data. We have set the upper altitude as the one for which the g-b data sensitivity reaches 50%. In other words, above that altitude, more than 50% of the information in the retrieved profiles comes from the a priori information, whereas below that altitude, at least 50% of the information comes from the FTIR measurement itself. This altitude is close to 30 km. The lowermost altitudes reached by the ACE-FTS profiles vary between 8

and 12 km above the sites concerned. In this range between 8 to 12 km and 30 km, the Degrees of Freedom for Signal (DOF) of the g-b FTIR profiles is close to 1. Therefore we will limit the comparisons to partial columns in the chosen altitude range, and not consider profiles.

Choosing the lower altitude for the partial columns is an exercise in compromise because the lower you fix the partial column lower boundary, the fewer ACE profiles you find that go down to this altitude. We have finally chosen the lower boundary at each site close to 12 km because this gives us the best compromise between (1) a sufficient number of co-incident ACE-FTS in order to have more reliable statistics, and (2), a DOF of the g-b FTIR partial columns in the range above that boundary up to the 50% sensitivity limit that is close to 1, and (3), an altitude that is similar at all sites. Izaña was the only site where we had to raise the lower boundary to 14.8 km, because there are only a few coincident profiles (ACE makes fewer observations in the tropics and extratropics than in the polar regions) and only two ACE-FTS profiles that go as low as 12 km. The finally chosen limits are listed in Table 3.

For each ACE-FTS profile, the partial column in the considered altitude range has been compared to the mean of the corresponding ones from the g-b FTIR profiles satisfying the coincidence criteria. To minimize the smoothing error (Rodgers and Connor, 2003), the ACE-FTS profile has first been smoothed with the g-b FTIR averaging kernel (after extrapolating the profile down to the surface using the a priori profile from the g-b FTIR retrieval). Figure 1 shows a correlation plot of the considered ACE-FTS versus ground-based FTIR partial column amounts for each contributing station.

Notice that the variation of the partial column amounts from one station to another is not a pure latitudinal variation: it is also linked to the fact that the altitude limits for the partial columns are not identical for all stations (see Table 3), and that the tropopause heights depend on latitude. In the end, the statistics of the partial column comparisons have been made for each site. These results are given in Table 3, together with some associated relevant information. The mean relative difference between the FTIR and ACE-FTS partial columns has been calculated as <ACE-FTS−FTIR>/<FTIR>. In Table 3, the standard error on the mean relative difference between the FTIR and ACE-FTS partial column (SEM, in percent) has been evaluated as STD/$\sqrt{N}$, in which STD is the statistical 1-sigma (1σ) standard deviation of the observed differences, and N is the number of coincidences. We will use SEM as a measure of the significance of an observed bias. The combined random error refers to the random error on the difference between the ACE-FTS and g-b FTIR partial columns, derived from the g-b FTIR random error covariance matrix and the ACE-FTS 1-sigma retrieval error provided with each profile (the ACE-FTS error covariance matrix is considered to be diagonal). The combined random error is expressed in percent, relative to the mean of the FTIR partial columns. The g-b FTIR random error covariance matrix has been evaluated for a typical FTIR measurement at Kiruna and has been adopted for all g-b FTIR profiles (F. Hase, private communication). More details about this latter evaluation and the procedure to calculate the random error on the partial column differences can be found in Vigouroux et al. (2007).

3.3 Comparison results

Inspection of Table 3 shows that, in the NH, there is a zero or small positive bias of the ACE-FTS partial columns between approximately 12 and 30 km compared to the g-b FTIR ones, except at Toronto. At the latter station, we see a negative bias of ACE-FTS of the order of $(-12.1\pm2.2)\%$; but the number of coincidences, 8, is rather poor and the g-b FTIR profiles seem to be less constrained (the DOF of the partial columns at Toronto is larger than it is at the other stations). Also at the northern subtropical station of Izaña, we observe a negative bias of ACE-FTS in the lower stratosphere of $(-6\pm3)\%$. In the SH, negative biases of ACE-FTS show up at all stations: they are of the order of -5% to -8%. At all sites, we see that the random error on the relative difference is smaller than the observed 1-sigma standard deviation, probably indicating that the coincidence criteria are too weak, and that we are still confronted with the variability in the actual CH_4 fields. However, taking into account, on average, the very low number of ACE-FTS overpasses, we have preferred not to strengthen the coincidence criteria.

From the limited number of coincidences, it is not possible given the statistics to draw any conclusion about any seasonal dependence in the differences between the ACE-FTS and g-b FTIR partial columns.

4 Comparison of ACE-FTS and SPIRALE profiles of CH_4

SPIRALE (French acronym for Spectroscopie Infra-Rouge d'Absorption par Lasers Embarqués) is a balloon-borne instrument operated by LPCE (CNRS-Université d'Orléans) and routinely used at all latitudes, in particular as part of European satellite validation campaigns for Odin and Envisat. The six tunable diode lasers absorption spectrometer (TDLAS) has been described in detail previously (Moreau et al., 2005). In brief it can perform simultaneous in situ measurements of about ten different long-lived and short-lived chemical species from about 10 to 35 km height, with a high frequency sampling (~1 Hz), thus enabling a vertical resolution of a few meters depending on the ascent rate of the balloon. The diode lasers emit in the mid-infrared domain (from 3 to 8 μm) with beams injected into a multipass Heriott cell located under the gondola and largely exposed to ambient air. The 3.5 m long cell is deployed during the ascent when the pressure is lower than 300 hPa. The multiple reflections obtained between the two cell mirrors give a total optical path of 430.78 m. Species concentrations are retrieved from direct infrared absorption, by fitting experimental spectra with spectra calculated using the HITRAN 2004 database (Rothman et al., 2005). Specifically, the ro-vibrational line at 1275.3868 cm^{-1} was used for CH_4 (a line not used by ACE-FTS). Measurements of pressure (using two calibrated and temperature-regulated capacitance manometers) and temperature (using two probes made of resistive platinum wire) aboard the gondola allow the conversion of the species concentrations into VMRs. Uncertainties in these parameters have been evaluated to be negligible regarding the other uncertainties discussed below. The global uncertainties in the VMRs have been assessed by taking into account the random errors and the systematic errors, and combining them as the square root of their quadratic sum. The random errors (fluctuations of the laser background emission signal and signal-to-noise ratio) and the systematic errors (laser line width and non-linearity of the detector) are very low, resulting in an estimated global uncertainty of 5% for CH_4, over the whole altitude range.

The SPIRALE measurements occurred on 20 January 2006, between 17:46 UT and 19:47 UT, with vertical profiles obtained during ascent, between 13.2 and 27.3 km height. The measurement position remained rather constant, at the balloon mean location of 67.6$\pm$0.2° N and 21.55$\pm$0.20° E. The comparison is made with the v2.2 data from the ACE-FTS sunrise sr13151 occultation that occurred 13 h later (on 21 January 2006 at 08:00 UT) and was located at 64.28° N, 21.56° E, i.e., 413 km away from the SPIRALE position. Using the MIMOSA contour advection model (Hauchecorne et al., 2002), PV maps in the region of both measurements have been calculated for each hour between 17:00 UT on 20 January and 08:00 UT on 21 January on isentropic surfaces, every 50 K from 400 K to 800 K (corresponding to 16–30 km

height). From these it was concluded that SPIRALE and ACE-FTS sounded similar air masses in the well-established polar vortex for the whole range of altitudes. The dynamical situation was very stable with a PV agreement better than 10%. So the geophysical situation was suitable for direct comparisons. In order to compare ACE-FTS and SPIRALE the difference in the vertical resolution of these two instruments had to be taken into account. Indeed, ACE-FTS has a vertical resolution of 3–4 km and that of SPIRALE is on the order of meters. A triangular convolution function of 3 km at the base (corresponding to the ACE-FTS vertical resolution) has been applied to the SPIRALE data. Consequently, the bottom and the top of SPIRALE profile have been truncated by 1.5 km. Then an interpolation onto the ACE-FTS 1 km-grid was performed.

Figure 2 shows that the ACE-FTS and SPIRALE CH$_4$ profiles are in good agreement below 24 km even if error bars do not overlap at the lowest altitudes (below 19 km). The observed relative differences over the altitude range of 15 to 24 km are smaller than 10%, with ACE-FTS values larger than SPIRALE except at 22.5 km. Above 24 km the relative differences increase, reaching 37% at 25.5 km, with ACE-FTS giving larger values than SPIRALE.

5 Comparisons between ACE-FTS and correlative MIPAS CH$_4$ profiles

The Michelson Interferometer for Passive Atmospheric Sounding (MIPAS) is an infrared limb-sounding Fourier transform interferometer on board the Envisat satellite, launched in March 2002 (Fischer et al., 2007). It acquires spectra over the range 685–2410 cm^{-1} (14.5–4.1 μm), which includes the vibration-rotation bands of many molecules of interest. It is capable of measuring continuously around each orbit during both day and night, and complete global coverage is obtained within 24 h.

From July 2002 until March 2004, MIPAS was operated at full spectral resolution (0.025 cm^{-1}) with a nominal limb-scanning sequence of 17 steps from 68 to 6 km with 3 km tangent height spacing in the troposphere and stratosphere, generating complete profiles spaced approximately every 500 km along the orbit. However, in March 2004 operations were suspended following problems with the interferometer slide mechanism. Operations were resumed in January 2005 with a 35% duty cycle and reduced spectral resolution (0.0625 cm^{-1}).

For the high-resolution part of the mission ESA has processed PT (pressure-temperature) and six "key species" (H$_2$O, O$_3$, HNO$_3$, CH$_4$, N$_2$O and NO$_2$). The algorithm used for the Level 2 analysis is based on the Optimised Retrieval Model (ORM) (Raspollini et al., 2006; Ridolfi et al., 2000). The spectroscopic database used in this retrieval is the so-called mipas_pf3.1 database (Flaud et al., 2003) which contains the same CH$_4$ line parameters as HITRAN 2004
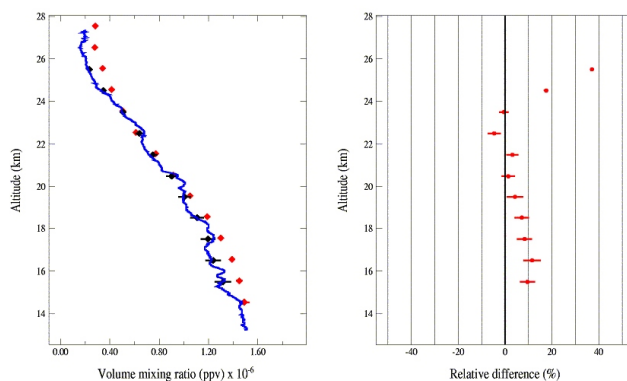

Fig. 2. Left plot: Methane vertical profiles obtained by ACE-FTS sr13151 (in red) and SPIRALE (in black and blue). The solid blue line corresponds to the SPIRALE measurements (very fine resolution) and the black diamonds correspond to the SPIRALE profile smoothed with a triangular convolution function (see Sect. 4). Error bars are reported on both profiles but, at several altitudes, they are so small that they are indiscernible. Right plot: The relative differences between the two profiles in percent, calculated as (200*(ACE-SPIRALE)/(ACE + SPIRALE)) and the corresponding error bars.
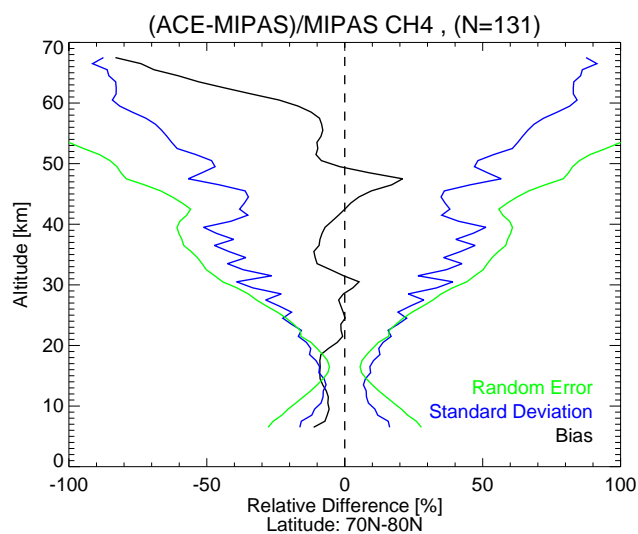
in the microwindows used by MIPAS. These windows are 1227.1750–1230.1750 cm^{-1} in the 6 to 60 km altitude range, and 1350.8750–1353.8750 cm^{-1} in the 12 to 68 km altitude range. The validation of the MIPAS operational v4.62 data processed by ESA is near completion (Espy and Hartogh, 2006; Piccolo and Dudhia, 2007), including a paper describing validation of CH$_4$ (Payan et al., 2007). The latter paper concludes, in part from comparisons with g-b FTIR data and HALOE profiles, that MIPAS overestimates the methane concentrations in the pressure range of 140 to 0.3 hPa ($\sim$15 to 58 km): on the global scale, the bias is of the order of 5 to 20%. The comparisons with HALOE show that the bias is largest at the upper and lower ends of the profiles. The observed biases with HALOE are however within the estimated combined systematic uncertainties, except at the highest altitudes (pressure <0.5 hPa).

In the present paper, MIPAS methane data v4.62 are compared with ACE-FTS version 2.2 data for the period from 21 February 2004 to 26 March 2004. During the first five months of the ACE mission, only sunsets were measured because of problems with spacecraft pointing at sunrise; therefore only NH data are available. The selected coincidence criteria were a maximum spatial and temporal difference of 300 km and 6 h, respectively. This slightly relaxed temporal mismatch (6 h) has been chosen in order to increase the statistics of the comparison, knowing that the species variability does not vary significantly when going from 3 to 6 h mismatch. So finally, the latitudinal coverage of the comparisons turns out to be limited to 70° N –80° N.
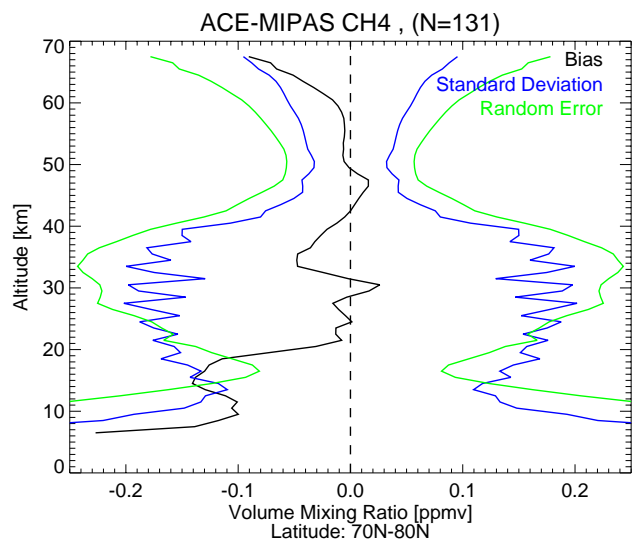
The comparison has been done including all the matching pairs (131) of measurements available in the considered
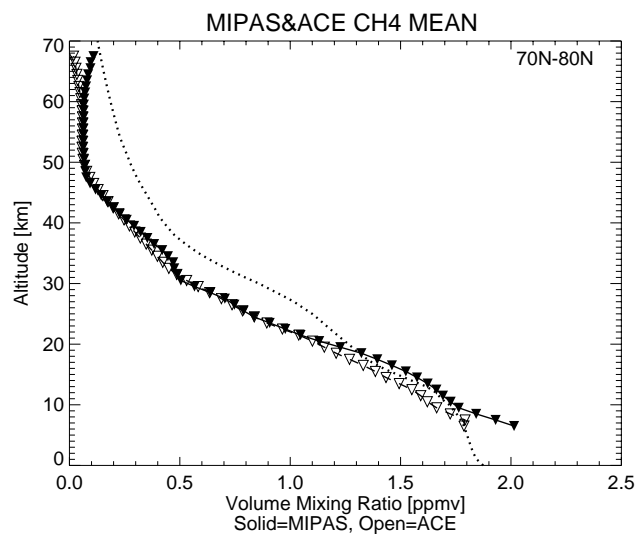
Fig. 3. Mean ACE-FTS (open triangles) and MIPAS (filled triangles) profiles of the 131 matching pairs in the 70–80° N latitude band, included in the comparison. The dotted line shows the MIPAS climatology (initial guess) for this latitude band.

Fig. 4. VMR difference between ACE-FTS and MIPAS profiles of CH$_4$: mean ACE-FTS minus MIPAS (black solid line) and associated 1σ standard deviation (blue solid line) for a sample of 131 coincident profiles in the 70 to 80° N latitude band. The random error of the difference profile, combining the MIPAS and ACE-FTS random errors, is shown as the green solid line.

period. Only the successfully retrieved points of the ACE-FTS profiles have been used in the comparison. Because the ACE-FTS profile above the highest analysed measurement is given as a scaled initial guess profile, it is not taken into account in the comparison. For MIPAS, only profiles associated with successful pressure/temperature and target species retrievals have been considered. It is useful to note that in

Fig. 5. Percentage relative difference between ACE-FTS and MIPAS profiles of CH$_4$: mean ACE-FTS minus MIPAS divided by MIPAS (black solid line) and associated standard deviation (blue solid line) for a sample of 131 coincident profiles in the 70 to 80° N latitude and ACE-FTS errors, is shown as the green solid line.

the operational MIPAS data negative VMR values have been truncated to 1.0×10^{-10}. These values have been filtered out from the profiles before making the comparison.

As far as MIPAS errors are concerned, we refer, in general, to the ESA level 2 products for the random error due to propagation of the instrument noise through the retrieval (Piccolo and Dudhia, 2007) and to results of the analysis carried out at University of Oxford for the systematic error (see data available at http://www-atm.physics.ox.ac.uk/group/mipas/err). Some of the components, listed in the Oxford University data set as systematic error on the individual profiles, show a random variability over the longer time-scale involved when averaging different MIPAS scans and/or orbits and tend to contribute to the standard deviation of the mean difference rather than to the bias. Taking this into account, for the present comparison with ACE-FTS, we have considered the error contribution due to propagation of pressure and temperature random covariance into the retrieval of key species VMR (taken from the Oxford Univ. data set) as a randomly variable component and combined it with the measurement noise – using the root-sums-square method – to obtain MIPAS random error.

Figures 3 to 5 show the comparison results on a statistical basis. Figure 3 includes the MIPAS climatological profile for the considered latitude band as a reference: this profile is taken from the MIPAS IG2 (initial guess) seasonal climatology by Remedios et al. (1999, 2007), and has been used in the ESA MIPAS data processing in the construction of the initial guess profile (Raspollini et al., 2006). From the mean of the 131 matching pairs of ACE-FTS and MIPAS profiles

between 10 and 70 km altitude shown in Fig. 3, one sees immediately a very good agreement at all altitudes, except below 21 km, between 32 and 40 km, and above 60 km. The differences ACE-FTS minus MIPAS are shown quantitatively in Figs. 4 and 5, in absolute units and percentages relative to MIPAS, respectively. Up to 60 km, the agreement looks very good, with relative differences that are within $\pm12\%$ except around 47 km where it rises to about 20%. If we consider the standard errors on the mean, defined as $\sigma/\sqrt{N}$ with σ the standard deviation and N the number of coincidences (131), as a measure of the significance of the bias, we find statistically significant negative biases between 8 and 20 km, of the order of $-10\%\pm1.5\%$, and between 32 and 40 km, of the order of $-10\%\pm5\%$. We find a statistically significant positive bias of about $19\%\pm5\%$ around 46–47 km. Above 50 km the bias becomes negative again, of order $-10\%\pm6\%$, and rises drastically above 60 km, up to $-80\%\pm8\%$. It has been verified that this large bias above 60 km is not due to the different sensitivity of MIPAS and ACE-FTS to non-local thermodynamic equilibrium (NLTE) conditions. Indeed, the emissions used in the MIPAS retrievals in the ν_4 band near 7.6 μm are in NLTE conditions during daytime above 50 km, reaching limb radiance deviations larger than 20% at 60 km and up to 60% at 70 km (López-Puertas et al., 2005), whereas the ACE-FTS absorptions are free of NLTE. But separate day- and nighttime comparisons show no significant differences as to the observed bias above 60 km. Above 60 km however, the random error on the MIPAS CH$_4$ profiles grows very large (from 10 to 60%) (Fig. 5 in Raspollini et al., 2006). The biases look compatible with the systematic uncertainty on the MIPAS profiles due to spectral database errors (Fig. 5 in Raspollini et al., 2006) that is of the same order of magnitude. Another reason for the high bias might be the truncation of negative VMR values in the operational MIPAS data that was mentioned above.

We also see that the standard deviation of the comparison is always smaller than the combined random error, as it should be, except in the range of 15 to 22 km altitude. This may be an indication of the fact that the variability in this altitude range in the dataset corresponds to high latitude northern winter-spring conditions, and is therefore too large within the chosen coincidence criteria.

6 Comparisons between ACE-FTS and correlative HALOE CH$_4$ profiles

6.1 Statistical analyses

A statistical analysis was performed to compare v2.2 CH$_4$ profiles from the ACE-FTS to v19 retrievals from HALOE onboard UARS. Like the ACE-FTS, HALOE is a solar occultation instrument, but the inclination of its orbit is 57°. Unlike ACE-FTS, HALOE is a filter channel spectrometer, that uses a gas filter correlation technique in the 3.3 μm re-
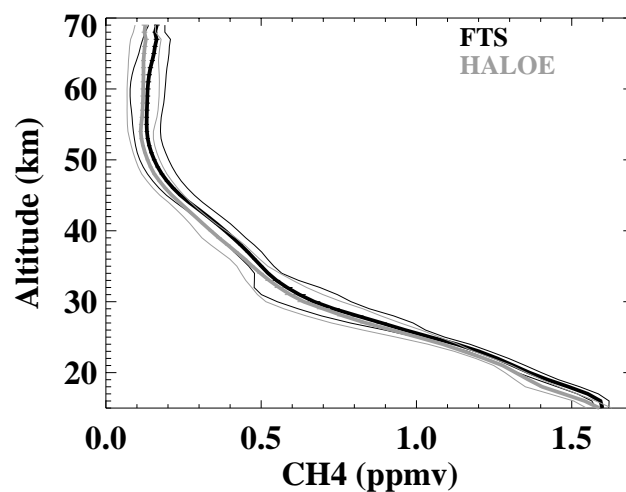

Fig. 6. Average profiles (thick lines) for all coincident measurements between ACE-FTS (black) and HALOE (gray). Thin lines are the profiles of standard deviations (1σ) of the distributions, while error bars (often too small to be seen) represent the uncertainty in the mean (σ divided by the square root of the number of comparisons).

gion (Russell et al., 1993). HALOE ceased operations in November 2005, so it operated throughout most of the first two years of the ACE mission. Version 17 HALOE CH$_4$ data were found to agree with correlative measurements to within about 15% in the stratosphere (Park et al., 1996). Comparisons between v19 HALOE and v1.0 ACE-FTS data were described by McHugh et al. (2005), who found that ACE-FTS CH$_4$ was about 10% higher than HALOE in the 18 to 55 km altitude range.

The HALOE and ACE-FTS v2.2 data sets were searched for coincident measurements, defined as occurring within 2 h in time and 500 km. ACE-FTS profiles with error bars larger than 100% have been discarded. A total of 36 coincidences were found; 5 of these corresponded to satellite sunrise (SR) occultations in both instruments, while the other 31 corresponded to satellite sunset (SS) occultations in both instruments. Opening up the time criterion to one day did not result in any new coincidences. The SS coincidences occurred from 4–10 July 2004 (29 coincidences, average latitude 66° N) and 15 August 2005 (2 coincidences, average latitude 49° S); the SR coincidences occurred on 6–7 September 2004 (5 coincidences, average latitude 60° N). Thus the majority of the comparisons correspond to polar summer conditions in the NH.

Figure 6 shows the average CH$_4$ profiles measured by both instruments for all coincidences. Although the analysis was performed separately for sunrise and sunset occultations, there were too few sunrise coincidences to obtain statistically significant results. Thus, only results for averages over all of the coincidences are reported here. Both instruments show very similar profile shapes, with the ACE-FTS mixing ratios
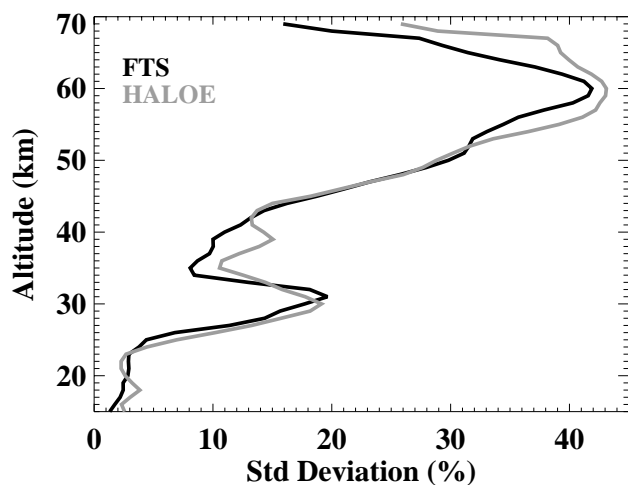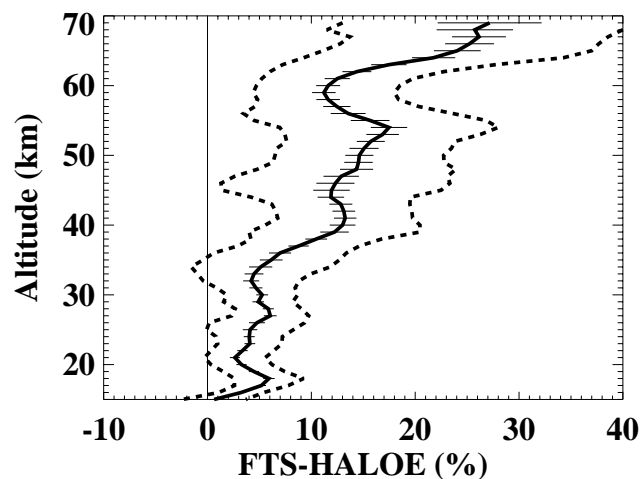
Fig. 7. Standard deviations of the distributions, 1σ, relative to the mean CH_4 mixing ratio at each altitude, for all coincident events, for ACE-FTS (black) and HALOE (gray).

Fig. 8. Average percent differences (solid) between ACE-FTS and HALOE relative to the average of the two instruments, for all coincidences. Dashed lines represent the 1σ standard deviation of the distribution of differences while the error bars represent the uncertainty in the mean difference, i.e., $\sigma/\sqrt{N}$ where N is the number of coincidences.

biased slightly high compared to HALOE, particularly above 35 km and below 25 km. At many altitudes the differences are accompanied by nearly overlapping error bars, suggesting that the differences are insignificant. Thin lines in Fig. 6 represent the standard deviations of the distribution of profiles measured by each instrument. Qualitatively, it is clear that both instruments measure similar variability.

Measurement variability is quantified more clearly in Fig. 7, which shows the standard deviations of the distributions relative to the mean mixing ratios. There is excellent agreement between ACE-FTS and HALOE at all altitudes, with both instruments capturing the local minimum in variability near 35 km, and maxima near 30 and 60 km. Hoppel et al. (1999) have shown evidence for summertime longitudinal variations in ozone from 21–28 km, at latitudes similar to those of the coincidences analyzed here. These variations arise from differential meridional transport caused by breaking of westward-propagating waves that are evanescent in the summer easterly flow. It is likely that this transport would also result in longitudinal variations in CH_4, thereby explaining the 30-km maximum in variability measured by both HALOE and ACE-FTS. A similar increase in variability is seen in the ACE-FTS HF and H_2O comparisons with HALOE (E. Mahieu and M. Carleer, respectively, private communication). Another contribution to the high variability at 30 km may be the chemical conversion between H_2O and CH_4: Nassar et al. (2005) noted that the variability in either CH_4 or H_2O was higher than the variability in $[H_2O]+2[CH_4]$.

Figure 8 shows the percent differences between the instruments, plotted as ACE-FTS minus HALOE relative to the average of the two instruments. As noted above, measurements from ACE-FTS are biased high compared to HALOE, with largest differences above 35 km. The overall agreement,

however, is excellent, with differences between the two instruments on the order of only 5% below 35 km, increasing to about 10–15% from 40–60 km. Overall, these results confirm that the ACE-FTS CH_4 measurements are on a par with the HALOE data, which have been used extensively for scientific analyses.

### 6.2 Comparisons in equivalent latitude/potential temperature space

ACE-FTS and HALOE CH_4 are compared here by mapping both fields in equivalent latitude (EqL)/potential temperature (θ) coordinates. The ACE and HALOE "Derived Meteorological Products" (DMPs) from the Met Office assimilated meteorological analyses are used to provide EqL/θ; these, and the mapping versus EqL, are described in detail by Manney et al. (2007). The mapping in EqL/θ is done as described by Manney et al. (1999, 2001) by taking weighted averages of the measurements around each EqL/θ gridpoint; in addition to being weighted by the "distance" (in EqL,θ) from the gridpoint, the average is weighted by the uncertainty value associated with the measurement point. The EqL grid spacing used is 5°, and the θ grid spacing corresponds to a 3-km grid, comparable to the vertical resolution of ACE-FTS and HALOE CH_4 profiles. EqL/time plots are produced in the same way, but gridding in time instead of θ. Time grid points are at 12:00 UT each day. The use of EqL as a coordinate allows us to compare measurements that are not spatially coincident, but were measured in the same air mass. Manney et al. (2007) showed that using EqL mapping to compare long-lived trace gases (such as CH_4) minimizes most biases

related to sampling differences in the EqL regions that are covered by both instruments.

Figure 9 shows the time evolution of ACE-FTS and HALOE CH_4 at 850 K (~10 hPa or 30 km) in the middle stratosphere from November 2004 through October 2005. The overlaid PV contours show the evolution of the polar vortices (solid contours are in vortex edge region). Because of the asymmetry and variability of the winter polar vortices, ACE-FTS measurements provide extensive coverage of conditions in and around the polar vortices. Very low CH_4 values in the vortices and very strong gradients across the vortex edge are the signature of strong, confined descent in the vortex (Schoeberl, et al., 1992 and references therein; Schoeberl et al., 1995; Manney et al., 1999); the close correspondence of the strong CH_4 gradient region in ACE-FTS with the evolution and position of the vortex-edge PV contours indicates good consistency of the ACE-FTS data with the meteorological fields.

ACE-FTS and HALOE measurements are rarely closely coincident in space and time. The general features of the evolution shown in Fig. 9 do, however, suggest good agreement in the overall time evolution of CH_4 from the two instruments, for example, the consistency in values, gradients and time changes along the Arctic vortex edge in November through March, similar high latitude values in summer in both hemispheres and in the equatorial regions. While close physical coincidences are few, during a typical month, HALOE and ACE-FTS cover many of the same EqL regions, indicating sampling of similar air masses. Figure 10 takes advantage of this for a more detailed comparison of ACE-FTS and HALOE, showing EqL/θ plots gridded as described above using all data from a month for November 2004, January 2005, June 2005, and September 2005. The signature of strong descent in the polar vortex is again apparent in ACE-FTS data for September in the SH, and in January in the NH; the NH November ACE-FTS fields show that much of the descent in the vortex region has already occurred by then, consistent with, e.g., Manney, et al. (2000). In November, the SH signature of strong descent is still apparent, but in the middle to upper stratosphere, strong mixing as the vortex breaks up has transported high CH_4 to high SH latitudes, while the lower stratospheric vortex is still strong; this pattern is consistent with that seen in MLS observations of N_2O and H_2O at this time (Manney et al., 2005). Differences between HALOE and ACE-FTS in regions of common coverage show good agreement in all periods shown. In November 2004 and January 2005, maximum differences are ~0.2 ppmv, and primarily localized, with no clear evidence of a consistent bias, other than a possible high bias of ACE-FTS with respect to HALOE of up to about 15% in January in the SH above ~1000 K (~35 km), and a slight low bias of ACE-FTS with respect to HALOE near 60° EqL above 700K (~30 km). Results for June are similar, except for a larger high ACE-FTS bias in the small EqL-coincident region in the NH upper stratosphere. There is also a slight low bias of ACE-FTS
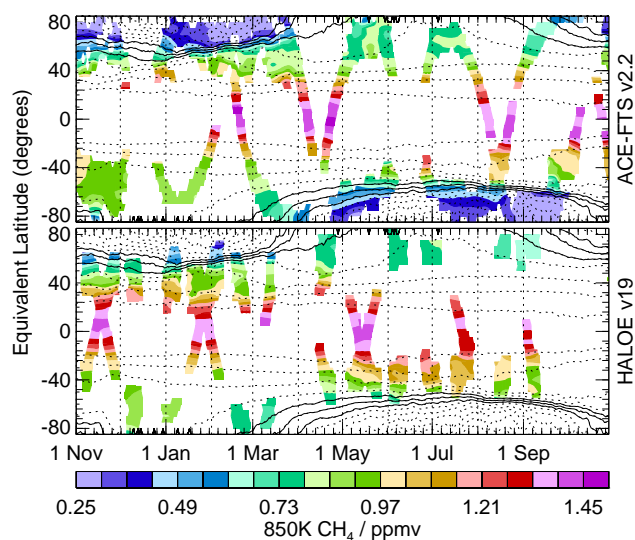

Fig. 9. ACE-FTS (top) and HALOE (bottom) CH4 VMR (ppmv) on the 850 K potential temperature surface as a function of equivalent latitude and time (see text) for November 2004 through October 2005. Overlaid contours are scaled PV from the Met Office meteorological analyses, with solid line showing contours demarking the polar vortex edge region.

with respect to HALOE above 700 K near −60° EqL, similar to that seen in the NH in January. These slight low ACE-FTS biases are along the vortex edge, and may thus be related to sampling effects, since in that region of very strong gradients, non-uniform sampling at different geographical latitudes may still affect EqL/θ results (Manney et al, 2007). The September results show slightly larger differences, with up to an ~25% high bias (still only ~0.2 ppmv) in much of the upper stratosphere, especially in the SH equatorward of −40° EqL. A slight high bias in the NH upper stratosphere is consistent with the analysis shown above in Sect. 6.1 of spatially coincident ACE-FTS and HALOE measurements. None of those coincidences were in the NH fall and winter periods represented by the November and January plots shown here, and the lack of a clear bias in these plots suggests that the HALOE/ACE-FTS differences may be seasonally-dependent and thus possibly related to atmospheric variability.

6.3 Consistency between both approaches

As pointed out above, one sees similar biases in summer high NH latitudes in both the (EqL/θ) (Sect. 6.2) and the statistical approach based on geographical coincidences (Sect. 6.1). It has been verified that the results of the statistical approach are robust with respect to EqL criteria.

The (EqL/θ) approach has a better global coverage in space and time, but it has the disadvantage that it is very difficult to identify whether an observed difference is statistically significant or not. The reason is that the value in a gridbox is derived from a different number of observations, and each of
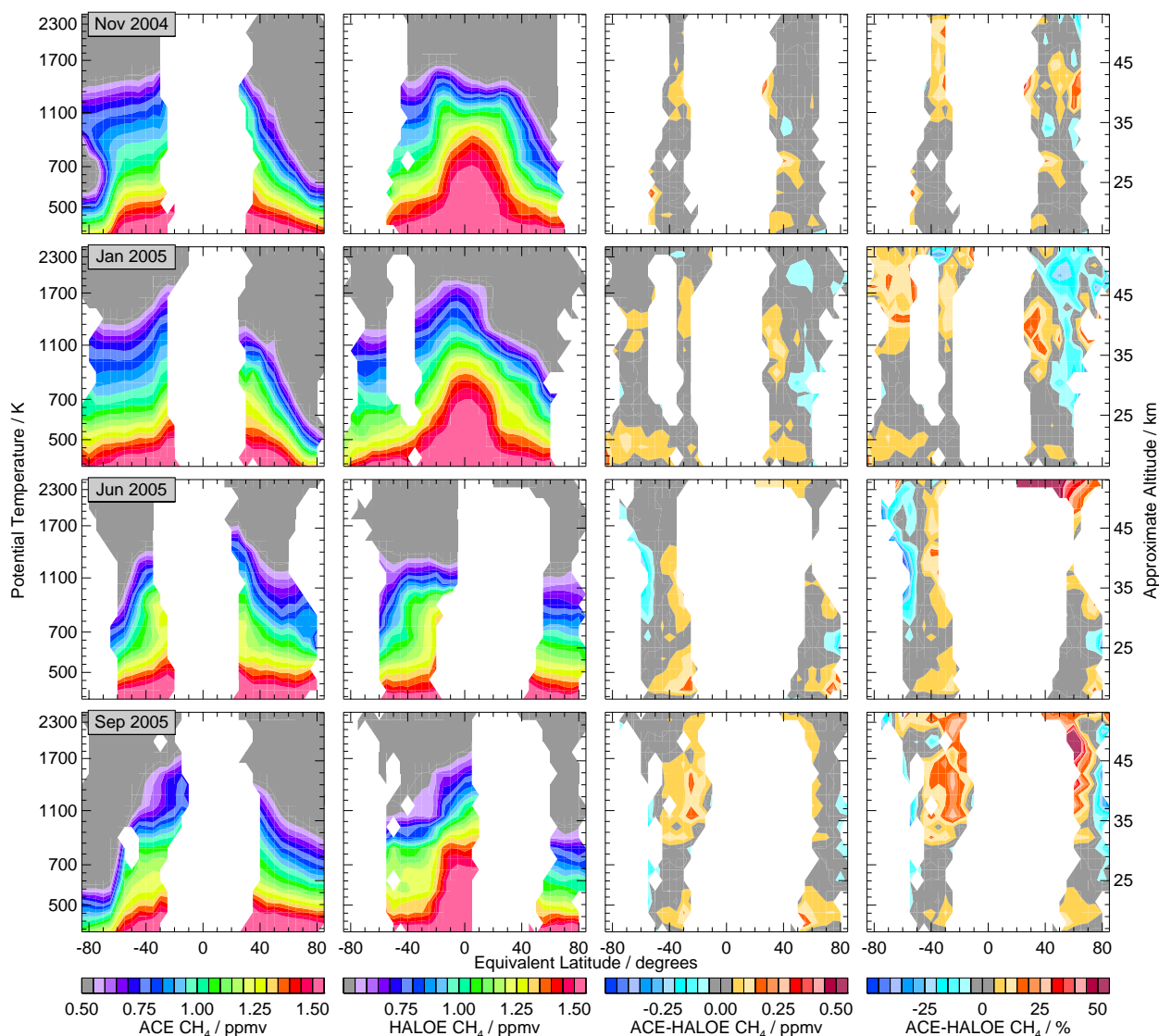
Fig. 10. Equivalent latitude/potential temperature (see text) sections of (left to right) ACE-FTS CH_4, HALOE CH_4, ACE-FTS−HALOE CH_4 in ppmv, and ACE-FTS−HALOE CH_4 in percent, for the months (from top to bottom) November 2004, January, June and September 2005. Vertical range is 400 K to 2500 K (15 to 50 km).

those is weighted differently according to its distance from the center of the gridbox and according to the uncertainties reported in the data files. So it is almost impossible to give a value above which the differences are significant. Because of this, (EqL/θ) mapping never provides a fully quantitative comparison.

Nevertheless, in the present study, it provides an indication of an ACE-FTS bias that has a latitudinal and seasonal dependence, and shows that in almost all cases, biases relative to HALOE are smaller than 25% in absolute value, leading to the conclusion that ACE-FTS and HALOE measurements of methane in the stratosphere-lower mesosphere are in good agreement.

7 Conclusions

7.1 Northern Hemisphere (NH)

In the high latitude NH, we have many comparisons in winter–spring namely one with a single SPIRALE profile in polar vortex conditions (67° N, January 2006), a statistical set of 131 MIPAS and ACE-FTS matched profiles in the 70–80° N latitude range between 21 February and 26 March 2004, and HALOE comparisons in (EqL/θ) space. We also have year-round comparisons with three ground-based stations. The results of these comparisons indicate that the ACE-FTS CH_4 VMR profiles are biased negative (of the order of −10%) with respect to MIPAS in the 8 to 20 km

altitude range, but positive (+10%) with respect to SPIRALE in a similar (15 to 20 km) altitude range. The comparisons of partial columns in the 12 to 25 km altitude range at the three high latitude ground-based stations also show a zero or slightly positive bias of the same order of magnitude. The comparisons with MIPAS and g-b FTIR seem to be consistent with the observation from Payan et al. (2007), mentioned in Sect. 5, that MIPAS has a high bias in this altitude range of the order of 5 to 20%.

At higher altitudes (stratosphere and lower mesosphere, up to 60 km), ACE-FTS CH_4 VMR profiles are in very good agreement with MIPAS. Above 60 km, the negative bias of ACE-FTS relative to MIPAS grows to −20%, but the errors on the individual MIPAS and ACE-FTS profiles become very high (larger than 30% for MIPAS).

The comparisons with HALOE do not cover the lowest altitude range, nor do they cover well the NH winter high latitude regions. But in NH high latitude summer conditions, comparisons with HALOE indicate that ACE-FTS has a positive bias of the order of 5 to 15% in the stratosphere, below and above 35 km, respectively. The bias rises to +30% above 65 km. If we presume that there is no seasonal variation in the bias in the high latitude NH, then this is consistent with the good agreement observed between ACE-FTS and MIPAS in this latitude and altitude range and the knowledge that MIPAS overestimates the methane compared to HALOE (Sect. 5, Payan et al., 2007).

Comparisons with HALOE do cover the NH winter mid-latitude regions, in which we observe a negative bias of ACE-FTS versus HALOE of the order of −5 to −25% in the stratosphere (>700 K or above ∼25 km). The comparisons with the NH mid-latitude and subtropical g-b FTIR stations (three stations in total) indicate a zero or negative bias of ACE-FTS of similar order of magnitude (−6 to −12%) in the lower stratosphere (<30 km).

7.2 Southern Hemisphere (SH)

The only comparisons in the SH consist of the comparisons with HALOE in (EqL/θ) space, and with ground-based FTIR stations. The former comparisons point to a slightly positive bias of ACE-FTS versus HALOE, of the order of 15% above 1000 K (∼35 km) in local summer high latitudes. The negative bias observed in NH mid-latitude in winter may also exist in SH mid-latitude winter.

In the lower stratosphere (12–30 km), the most reliable, from a statistical point of view, comparisons with g-b FTIR data indicate a slightly negative bias of ACE-FTS (of the order of −5 to −8%) at southern mid-latitudes.

7.3 General conclusions

Overall one can say from the analyses of ACE-FTS CH_4 VMR profiles in (EqL/θ) space and their comparisons with HALOE, that the ACE-FTS data in the stratosphere are consistent with the meteorological fields. They also reproduce the variability of atmospheric methane very well. Based on the available comparisons with independent correlative data, we can also say that the ACE-FTS CH_4 data have an overall accuracy that is within 10% in the upper troposphere – lower stratosphere, and within 25% in the middle and higher stratosphere up to the lower mesosphere (<60 km). The observed biases are small and consistent with reported systematic uncertainties, to which the spectroscopic uncertainties are a large contribution. There are also indications for some seasonal and latitudinal dependence in the differences between ACE-FTS and correlative data.

References

Abrams, M. C., Chang, A. Y., Gunson, M. R., Abbas, M. M., Goldman, A., Irion, F. W., Michelsen, H. A., Newchurch, M. J., Rinsland, C. P., Stiller, G. P., and Zander, R.: On the assessment and uncertainty of atmospheric trace gas burden measurements with high-resolution infrared solar occultation spectra from space by the ATMOS experiment, Geophys. Res. Lett., 23, 2337–2340, 1996.

Barnet, C., Datta, S., and Strow, L.: Trace gas measurements from the Atmospheric Infrared Sounder (AIRS), in Optical Remote Sensing (Trends in Optics and Photonics Series Vol. 85), 89–92, 2003.

Bernath, P. F., McElroy, C. T., Abrams, M. C., et al.: Atmospheric Chemistry Experiment (ACE): Mission overview, Geophys. Res. Lett., 32, L15S01, doi:10.1029/2005GL022386, 2005.

Boone, C. D., R. Nassar, K. A. Walker, Y. Rochon, S. D. McLeod, C. P. Rinsland, and Bernath, P. F. : Retrievals for the atmospheric chemistry experiment Fourier-transform spectrometer, Appl. Optics, 44 (33), 7218–7231, 2005.

Brasseur, G. P., Orlando, J. J., and Tyndall, G. S.: Atmospheric Chemistry and Global Change, Oxford University Press (New York, Oxford), 1999.

Espy, P. J. and Hartogh, P.: MIPAS: Potential of the experiment, data processing and validation of results, Special Issue in Atmos. Chem. Phys., 2006.

Fischer, H., Birk, M., Blom, C., Carli, B., Carlotti, M., von Clarmann, T., Delbouille, L., Dudhia, A., Ehhalt, D., Endemann, M., Flaud, J. M., Gessner, R., Kleinert, A., Koopman, R., Langen, J., Lpez-Puertas, M., Mosner, P., Nett, H., Oelhaf, H., Perron, G., Remedios, J., Ridolfi, M., Stiller, G., and Zander, R.: MIPAS: an instrument for atmospheric and climate research, Atmos. Chem. Phys., 8, 2151–2188, 2008,
http://www.atmos-chem-phys.net/8/2151/2008/.

Frankenberg, C., Meirink, J. F., van Weele, M., Platt, U., and Wagner, T.: Assessing methane emissions from global space-borne observations: Science, 308, 1010–1014, doi:10.1126/science.1106644, 2005.

GLOBALVIEW-CH4: Cooperative Atmospheric Data Integration Project – Methane. CD-ROM, NOAA ESRL, Boulder, Colorado; also available on Internet at http://www.esrl.noaa.gov/gmd/ccgg/globalview/ch4/ch4_intro.html, 2005.

Gunson, M. R., Farmer, C. B., Norton, R. H., Zander, R., Rinsland, C. P., Shaw, J. H., and Gao, B. C.: Measurements of CH_4, N_2O, CO, H_2O, and O_3 in the middle atmosphere by the ATMOS experiment on Spacelab 3, J. Geophys. Res., 95, 13 867–13 882, 1990.

Gunson, M. R., Abbas, M. M., Abrams, M. C., et al.: The Atmospheric Trace Molecule Spectroscopy (ATMOS) experiment: Deployment on the ATLAS Space Shuttle missions, Geophys. Res. Lett., 23, 2333–2336, 1996.

Hase, F., Hannigan, J. W., Coffey, M. T., Goldman, A., Höpfner, M., Jones, N. B., Rinsland, C. P., and Wood, S. W.: Intercomparison of retrieval codes used for the analysis of high-resolution, ground-based FTIR measurements, J. Quant. Spectrosc. Ra. Trans., 87, 25–52, 2004.

Hauchecorne, A., Godin, S., Marchand, M., Heese, B., and Souprayen, C.: Quantification of the transport of chemical constituents from the polar vortex to midlatitudes in the lower stratosphere using the high-resolution advection model MIMOSA and effective diffusivity, J. Geophys. Res., 107, 8289, doi:10.1029/2001JD000491, 2002.

Hoppel, K. W., Bowman, K. P., and Bevilacqua, R. M.: Northern Hemisphere summer ozone variability observed by POAM II, Geophys. Res. Lett., 26, 827–830, 1999.

López-Puertas, M., Funke, B., Gil-López, S., López-Valverde, M. A., von Clarmann, T., Fischer, H., Oelhaf, H., Stiller, G., Kaufmann, M., Koukouli, M. E., and Flaud, J.-M.: Atmospheric non-local thermodynamic equilibrium emissions as observed by the Michelson Interferometer for Passive Atmospheric Sounding (MIPAS), C.R. Physique, Elsevier SAS, 6, 848–862, 2005.

Manney, G. L., Michelsen, H. A., Santee, M. L., Gunson, M. R.,

Irion, F. W., Roche, A. E., and Livesey, N. J.: Polar vortex dynamics during spring and fall diagnosed using trace gas observations from the Atmospheric Trace Molecule Spectroscopy instrument, J. Geophys. Res., 104, 18 841–18 866, 1999.

Manney, G. L., Michelsen, H. A., Irion, F. W., Gunson, M. R., Toon, G. C., and Roche, A. E.: Lamination and polar vortex development in fall from ATMOS long-lived trace gases observed during November 1994, J. Geophys. Res., 105, 29 023–29 038, 2000.

Manney, G. L., Michelsen, H. A., Bevilacqua, R. M., Gunson, M. R., Irion, F. W. Livesey, N. J., Oberheide, J., Riese, M., Russell III, J. M., Toon, G. C., and Zawodny, J. M.: Comparison of satellite ozone observations in coincident air masses in early November 1994, J. Geophys. Res., 106, 9923–9944, 2001.

Manney, G. L., Santee, M. L., Livesey, N. J., Froidevaux, L., Read, W. G., Pumphrey, H. C., Waters, J. W., and Pawson, S.: EOS Microwave Limb Sounder observations of the Antarctic polar vortex breakup in 2004, Geophys. Res. Lett., 32, L12811, doi:10.1029/2005GL022823, 2005.

Manney, G. L., Daffer, W. H., Zawodny, J. M., Bernath, P. F., Hoppel, K. W., Walker, K. A., Knosp, B. W., Boone, C., Remsberg, E. E., Santee, M. L., Lynn Harvey, V., Pawson, S., Jackson, D. R., Deaver, L., McElroy, C. T., McLinden, C. A., Drummond, J. A., Pumphrey, H. C., Lambert, A., Schwartz, M. J., Froidevaux, L., McLeod, S., Takacs, L. L., Suarez, M. J., Trepte, C. R., Cuddy, D. T., Livesey, N. J., Harwood, R. S., and Waters, J. W.: Solar Occultation Satellite Data and Derived Meteorological Products: Sampling Issues and Comparisons with Aura MLS, J. Geophys. Res., 112, D24S50, doi:10.1029/2007JD008709, 2007.

McHugh, M., Magill, B., Walker, K. A., Boone, C. D., Bernath, P. F., and Russell, III, J. M.: Comparison of atmospheric retrievals from ACE and HALOE, Geophys. Res. Lett. 32, L15S10, doi:10.1029/2005GL022403, 2005.

Mondelain, D., Payan, S., Deng, W., Camy-Peyret, C., Hurtmans, D., and Mantz, A. W.: Measurement of the temperature dependence of line mixing and pressure broadening parameters between 296 and 90 K in the ν_3 band of $^{12}CH_4$ and their influence on atmospheric methane retrievals, J. Mol. Spectrosc., 244, 130–137, 2007.

Moreau, G., Robert, C., Catoire, V., Chartier, M., Camy-Peyret, C., Huret, N., Pirre, M., Pomathiod, L., and Chalumeau, G.: SPIRALE: a multispecies in situ balloon-borne instrument with six tunable diode laser spectrometers, Appl. Opt., 44(28), 5972–5989, 2005.

Nassar, R., Bernath, P. F., Boone, C. D., Manney, G. L., McLeod, S. D., Rinsland, C. P., Skelton, R., and Walker, K. A.: Stratospheric abundances of water and methane based on ACE-FTS measurements, Geophys. Res. Lett., 32, L15S04, doi:10.1029/2005GL022383, 2005.

Park, J. H., Russell III, J. M., Gordley, L. L., Drayson, S. R., Benner, D. C., McInerney, J. M., Gunson, M. R., Toon, G. C., Sen, B., Blavier, J.-F., Webster, C. R., Zipf, E. C., Erdman, P., Schmidt, U., and Schiller, C.: Validation of Halogen Occultation Experiment CH_4 measurements from the UARS, J. Geophys. Res., 101(D6), 10 183–10 203, 1996.

Payan, S., Camy-Peyret, C., Oelhaf, H., Wetzel, G., Maucher, G., Kleim, C., Pirre, M., Huret, N., Engel, A., Volk, M. C., Kuellmann, H., Kuttippurath, J., Cortesi, U., Bianchini, G., Mencaraglia, F., Raspollini, P., Redaelli, G., Vigouroux, C., De Mazire, Mikuteit, S., Blumenstock, T., Velazco, V., Notholt, J., Mahieu,

M., Duchatelet, P., Smale, D., Wood, S., Jones, N., M., Piccolo, C., Payne, V., Bracher, A., Glatthor, N., Stiller, G., Grunow, K., Jeseck, P., Ye, T., Pfeilsticker, K., and Butz, A.: Validation and data characteristics of methane and nitrous oxide profiles observed by MIPAS and processed with Version 4.61 algorithm, Atmos. Chem. Phys. Discuss., 7, 18043–18111, 2007, http://www.atmos-chem-phys-discuss.net/7/18043/2007/.

Piccolo, C. and Dudhia, A.: Precision validation of MIPAS-Envisat products, Atmos. Chem. Phys., 7, 1915–1923, 2007, http://www.atmos-chem-phys.net/7/1915/2007/.

Raspollini, P., Belotti, C., Burgess, A., Carli, B., Carlotti, M., Ceccherini, S., Dinelli, B. M., Dudhia, A., Flaud, J.-M., Funke, B., Höpfner, López-Puertas, M., Payne, V., Piccolo, C., Remedios, J. J., Ridolfi, M., and Spang, R.: MIPAS level 2 operational analysis, Special Issue MIPAS: Potential of the experiment, data processing and validation of results, edited by: Espy, P. J. and Hartogh, P., Atmos. Chem. Phys., 6, 5605–5630, 2006, http://www.atmos-chem-phys.net/6/5605/2006/.

Reber, C. A., Trevathan, C. E., McNeal, R. J., and Luther, M. R.: The Upper Atmosphere Research Satellite (UARS) mission, J. Geophys. Res., 98, 10 643–10 647, doi:10.1029/92JD02828, 1993.

Remedios, J. J., Ruth, S. L., Rodgers, C. D., Taylor, F. W., Roche, A. E., Gille, J. C., Gunson, M. R., Russell III, J. M., Park, J., Zipf, E. C., and Erdman, P. W.: Measurements of methane and nitrous oxide distributions by the improved stratospheric and mesospheric sounder: Retrieval and validation, J. Geophys. Res., 101, 9843–9871, 1996.

Remedios, J. J.: Extreme Atmospheric Constituent Profiles for MIPAS, Proceedings of the European symposium on atmospheric measurements from space, ESTEC, Netherlands, 20–22 January, 2, 779–783, 1999.

Remedios, J. J., Leigh, R. J., Waterfall, A. M., Moore, D. P., Sembhi, H., Parkes, I., Greenhough, J., Chipperfield, M. P., and Hauglustaine, D.: MIPAS reference atmospheres and comparisons to V4.61/V4.62 MIPAS level 2 geophysical data sets, Special Issue "MIPAS: Potential of the experiment, data processing and validation of results", edited by: Espy, P. J. and Hartogh, P., Atmos. Chem. Phys. Discuss., 7, 9973–10017, 2007, http://www.atmos-chem-phys-discuss.net/7/9973/2007/.

Ridolfi, M., Carli, B., Carlotti, M., von Clarmann, T., Dinelli, B. M., Dudhia, A., Flaud, J.-M., Höpfner, M., Morris, P. E., Raspollini, P., Stiller, G., and Wells, R. J.: Optimized forward model and retrieval scheme for MIPAS near-real-time data processing, Appl. Opt., 39, 1323–1340, 2000.

Roche, A. E.,Kumer, J. B., Nightingale, R. W., Mergenthaler, J. L., Ely, G. A., Bailey, P. L., Massie, S. T., Gille, J. C., Edwards, D. P., Gunson, M. R., Abrams, M. C., Toon, G. C., Webster, C. R., Traub, W. A., Jucks, K. W., Johnson, D. G., Murcray, D. G., Murcray, F. H., Goldman, A., and Zipf, E. C.: Validation of CH_4 and N_2O measurements by the CLAES instrument on the Upper Atmospheric Research Satellite, J. Geophys. Res., 101, 9679–9710, 1996.

Rodgers, C. D.: Inverse methods for atmospheric sounding: Theory and Practice, Series on Atmospheric, Oceanic and Planetary Physics, 2, World Scientific Publishing Co., Singapore, 2000.

Rodgers, C. D. and Connor, B. J.: Intercomparison of remote sounding instruments, J. Geophys. Res., 108, 4116–4129, 2003.

Rothman, L. S., Jacquemart, D., Barbe, A., Chris Bennerc, D., Birk, M., Brown, L. R., Carleer, M. R., Chackerian Jr., C., Chance, K., Coudert, L. H., Dana, V., Devi, V .M., Flaud, J.-M., 30 Gamache, R. R., Goldman, A., Hartmann, J.-M., Jucks, K. W., Maki, A. G., Mandin, J.-Y., Massie, S. T., Orphal, J., Perrin, A., Rinsland, C. P., Smith, M. A. H., Tennyson, J., Tolchenov, R. N., Toth, R. A., Vander Auwera, J., Varanasi, P., and Wagner, G.: The HITRAN 2004 molecular spectroscopic database, J. Quant. Spectrosc. Ra. Trans., 96, 139–204, 2005.

Russell, J. M., III, Gordley, L. L., Park, J. H., Drayson, S. R., Tuck, A. F., Harries, J. E., Cicerone, R. J., Crutzen, P. J., and Frederick, J. E.: The Halogen Occultation Experiment, J. Geophys. Res., 98, 10 777–10 797, 1993.

Schoeberl, M. R., Lait, L. R., Newman, P. A., and Rosenfield, J. E.: The structure of the polar vortex, J. Geophys. Res., 97, 7859–7882, 1992.

Schoeberl, M. R., Luo, M., and Rosenfield, J. E.: An analysis of the Antarctic Halogen Occultation Experiment trace gas observations, J. Geophys. Res., 100, 5159–5172, 1995.

Vigouroux, C., De Mazière, M., Errera, Q., Mahieu, E., Duchatelet, P., Wood, S., Smale, D., Mikuteit, S., Blumenstock, T., Hase, F., and Jones, N.: Comparisons between ground-based FTIR and MIPAS N_2O and HNO_3 profiles before and after assimilation in BASCOE, Atmos. Chem. Phys., 7, 377–396, 2007, http://www.atmos-chem-phys.net/7/377/2007/.

Wahlen, M.: The Global Methane Cycle, Annu. Rev. Earth Pl. Sc., 21, 407–426, 1993.